Behavioral/Cognitive

Fear from the Heart: Sensitivity to Fear Stimuli Depends on Individual Heartbeats

Sarah N. Garfinkel,[1,2] Ludovico Minati,[1,3] Marcus A. Gray,[4] Anil K. Seth,[2,5] Raymond J. Dolan,[6] and Hugo D. Critchley[1,2]

[1]Department of Psychiatry, Brighton and Sussex Medical School, and [2]Sackler Centre for Consciousness Science, University of Sussex, Falmer BN1 9RR, United Kingdom, [3]Scientific Department, Fondazione IRCCs Instituto Neurologico Besta, 20133 Milan, Italy, [4]Centre for Advanced Imaging, The University of Queensland, Brisbane St Lucia QLD 4072, Australia, [5]Department of Informatics, University of Sussex, Falmer BN1 9QJ, United Kingdom, and [6]Wellcome Trust Centre for Neuroimaging, University College London, London WC1N 3BG, United Kingdom

Cognitions and emotions can be influenced by bodily physiology. Here, we investigated whether the processing of brief fear stimuli is selectively gated by their timing in relation to individual heartbeats. Emotional and neutral faces were presented to human volunteers at cardiac systole, when ejection of blood from the heart causes arterial baroreceptors to signal centrally the strength and timing of each heartbeat, and at diastole, the period between heartbeats when baroreceptors are quiescent. Participants performed behavioral and neuroimaging tasks to determine whether these interoceptive signals influence the detection of emotional stimuli at the threshold of conscious awareness and alter judgments of emotionality of fearful and neutral faces. Our results show that fearful faces were detected more easily and were rated as more intense at systole than at diastole. Correspondingly, amygdala responses were greater to fearful faces presented at systole relative to diastole. These novel findings highlight a major channel by which short-term interoceptive fluctuations enhance perceptual and evaluative processes specifically related to the processing of fear and threat and counter the view that baroreceptor afferent signaling is always inhibitory to sensory perception.

Key words: **amygdala; anxiety; attention; baroreceptor; emotion; fMRI**

Introduction

The internal state of the body influences our perceptions, cognitions, and emotions. However, the specific neural mechanisms have yet to be elucidated. "Peripheral" theories of emotion emphasize the centrality of bodily responses to subjective experience of emotion. Emotional feelings are proposed to arise from the occurrence of physiological change and appraisal of its generating context (James, 1890/1950; Lange, 1885; Schachter and Singer, 1962; Seth, 2013). Signals from the body, including movement of facial muscles, can feedback to bias emotional judgments (Strack et al., 1988). Increasingly, a dynamic relationship is recognized between internal physiological state and cognition, in which changes in bodily arousal affect decision making and memory (Bechara et al., 2000; Garfinkel et al., 2013).

Brain areas implicated in the generation and representation of bodily arousal also support emotional and attentional processes. These include anterior cingulate, insula, amygdala, and specific brainstem nuclei (Fredrikson et al., 1998; Zhang et al., 1998; Gray et al., 2007b). Among these, the amygdala is particularly linked to the processing of threat (LeDoux, 2000), whereas its activation also mediates enhanced memory of emotional information (Cahill and McGaugh, 1998) and arousal-induced attentional capture (Anderson and Phelps, 2001). Physiological arousal and amygdala hyperactivation are a feature of anxiety disorders, notably posttraumatic stress disorder (PTSD), in which heightened threat perception accompanies a sense of proximal danger (Garfinkel and Liberzon, 2009). Conversely, individuals with peripheral autonomic denervation show reduced amygdala responses to threat stimuli, suggesting that this region, along with the "interoceptive" insular cortex, is sensitive to viscerosensory feedback (Critchley et al., 2002a).

One experimental strategy to assess how bodily arousal influences cognitive and emotional processes is to capitalize on naturally occurring bodily fluctuations such as cardiovascular rhythmicity (Edwards et al., 2008; Gray et al., 2009). In the cardiac cycle, the strength and timing of individual heartbeats is encoded by bursts of afferent neural activity from arterial baroreceptors to brainstem during systole (the ventricular ejection period). This afferent signal is of primary importance to the baroreflex control of blood pressure, yet it also interacts with other types of sensory processing: Nociception can be attenuated during systole (Edwards et al., 2002) and facial expressions of disgust may be judged as more intense when presented at systole relative to diastole (Gray et al., 2012). Similarly, electrocutaneous shocks presented at diastole and systole are as-

Received Aug. 14, 2013; revised Feb. 28, 2014; accepted March 9, 2014.

Author contributions: S.N.G., R.J.D., and H.D.C. designed research; S.N.G. performed research; S.N.G., L.M., and H.D.C. analyzed data; S.N.G., L.M., M.A.G., A.K.S., R.J.D., and H.D.C. wrote the paper.

This work was supported by the Dr. Mortimer and Theresa Sackler Foundation. H.D.C. and S.N.G. are supported by the European Research Council (Advanced Grant CCFIB AG 234150 to H.D.C.). R.J.D. is supported by the Wellcome Trust. A.K.S. is supported by the European Union (Project CEEDS FP7-ICT-2009-05, 258749) and the Engineering and Physical Sciences Research Council Leadership (Fellowship EP/G007543/1). We thank Duncan Fowler and Cassandra Gould for technical assistance.

The authors declare no competing financial interests.

This article is freely available online through the *J Neurosci* Author Open Choice option.

Correspondence should be addressed to Sarah N Garfinkel, Clinical Imaging Science Centre, Brighton and Sussex Medical School, University of Sussex, Falmer BN1 9RR, UK. E-mail: s.garfinkel@bsms.ac.uk.

DOI:10.1523/JNEUROSCI.3507-13.2014

 0270-6474/14/346573-10$15.00/0

sociated with distinct neural signatures, with enhanced amygdala activation observed to shocks at systole (Gray et al., 2009). However, this type of cardiac-timing paradigm has not previously been applied to assess alterations in subjective, behavioral, and neural anatomical indices of fear processing.

Bodily states of arousal are particular relevant to fear and anxiety. Fear states are strongly coupled to sympathetic nervous activation and highly anxious individuals manifest increased sensitivity to psychological threat that translates into enhanced autonomic reactivity (Metzger et al., 1999; Tsunoda et al., 2008) and superior detection of internal bodily sensations, notably heartbeats (Domschke et al., 2010). Here, we report findings of two experiments that explored cardiac-timing effects on fear perception and fear judgment.

Materials and Methods

Experiments. In a first experiment, we examined behaviorally how the cardiac cycle alters the detection and attentional capture of threat stimuli at the limit of conscious perceptual awareness (Experiment 1). We used an emotional attentional blink paradigm time locked to specific phases of the cardiac cycle and quantified the detection breakthrough of emotional stimuli (fear, happy, disgust, and neutral faces). To maximize power to detect the impact of cardiac cycle on attentional breakthrough, we chose a threshold that was located within the "blink" period, which is on the cusp of conscious detection (Anderson and Phelps, 2001; De Martino et al., 2009). In Experiment 2, which was performed during functional neuroimaging, we tested for cardiac-induced alterations in the subjective emotional intensity of explicit fear and neutral stimuli while assessing underlying neural substrates. We specifically tested the hypothesized role of the amygdala in mediating heart-timing effects on fear processing. Individual differences in anxiety were used to investigate whether they affect cardiac modulation of fear intensity ratings.

Participants. Both studies were approved by the Brighton and Sussex Medical School Research Governance and Ethics Committee. Healthy control participants were recruited from advertisements posted on community websites and around campus. For Experiment 1, 23 participants took part (15 females, eight males); three were removed from analyses because of synchronization failure of the equipment used for heart timing and one was excluded because of resting tachycardia (110 bpm at rest). The mean age of participants was 26.7 ± 8.6 years. For Experiment 2, a separate cohort of participants underwent structured independent screening for health problems before MRI scanning, resulting in 19 healthy control participants (seven females, 12 males). The mean age of participants was 28.2 ± 5.4 years. All participants provided informed consent.

Detection of heartbeat. Physiological waveforms were recorded on PC (power 1401, Spike2 v7 software; CED). For Experiment 1, cardiac cycle was ascertained using electrocardiography (ECG) and, for Experiment 2, which took place in the MRI scanner, heartbeats were monitored using MRI-compatible finger pulse oximetry (8600Fo; Nonin Medical). Following calibrations made in previous studies, using similar methods and recruiting from the same population, an estimated mean pulse transit time of ~200 ms was used (Gray et al., 2012). Physiological waveforms were recorded on PC (power 1401, Spike2 v7 software; CED). Timing of stimulus presentation was controlled by a real-time script running on the CED-power1401 unit, identifying the QRS complex with millisecond temporal accuracy. Stimulus presentation was time locked to either the R-wave (end of cardiac diastole) or delayed ~300 ms from the R-wave peak to coincide with the T-wave at systole, when baroreceptor impulses are processed centrally (Edwards et al., 2007; Edwards et al., 2009; Gray et al., 2009). See Figure 1*A* for a histogram detailing the precision of face stimulus presentation in relation to cardiac cycle in the MRI scanner.

Stimuli. Face stimuli were taken from the Karolinska Directed Emotional Faces: (Lundqvist et al., 1998) and the Ekman set (Ekman and Friesen, 1974). Experiment 1 included 60 fear, 60 disgust, 60 happy, and 90 neutral faces. Experiment 2 focused on fear and neutral faces only (40 fear, 40 neutral) as the key stimuli of interest. The attentional blink paradigm (Experiment 1) also included stimuli comprised of buildings (both inside and outside), which were adapted from digital catalogs displaying houses and rooms. All pictures were grayscale and standardized to form 305 × 305 squares. Distractor images were comprised of scrambled images formed of two face and house stimuli randomly chosen on a trial by trial basis. For each trial, these were fractured into 25 squares (5 × 5) and "scrambled" together through random shuffling to form 13 unique composite images.

Paradigms and procedure. For Experiment 1, a behavioral attentional blink paradigm using pictures (De Martino et al., 2009) was modified to ensure that the rapid serial visual presentation (RSVP) was time locked to either the R-wave (end of cardiac diastole) or delayed ~300 ms from the R-wave peak to coincide with the T-wave at systole, when baroreceptor impulses are processed centrally (Edwards et al., 2007; Edwards et al., 2009; Gray et al., 2009). Each participant performed 180 trials, formed of 60 neutral, 40 fear, 40 disgust, and 40 happy face presentations, half of which were presented at diastole, half at systole. RSVPs were comprised of 13 scrambled "mask" items, an initial target (T1), which always depicted an image of a house, either inside or outside, and a second target (T2), which was always a face (fear, disgust, neutral, or happy). T2 served as our variable of interest and T1 acted as a control stimulus. During the RSVP, these 15 items (13 scrambled, T1, and T2) appeared on the screen for 70 ms each. To ensure that an attentional blink masking effect was optimized (De Martino et al., 2009), in the majority of trials (>80%), the T2 was presented 5 items after the T1. The placement of the T1 and T2 items were randomized on a within-participant basis, with T1 presented as item 3, 5, or 7 and T2 on respective trials presented as item 8, 10, or 12. All mask items were formed of a house and face item chosen from a fully randomized database and scrambled "online" on a trial-by-trial basis (Fig. 1*B*). Therefore, each trial lasted 1050 ms, during which the participant attended to a stream of largely scrambled pictures and attempted to perceive a house and a face stimulus. Each trial was immediately followed by a test phase in which the participant was required to make recognition decisions regarding which T1 (house) and which T2 (face) was presented. Once for the T1 identification and once for T2 identification, the participant was presented with three options composed of the target and two distractor stimuli of the same class (i.e., if T1 was an outdoor house, distractor items were also outdoor images of houses). The participant was required to make a forced choice, denoting which target stimulus was presented in the preceding RSVP. Because this study was concerned with cardiac modulation of emotional processing, all results focus on the masked T2 face stimuli.

For Experiment 2, which took place in the MRI scanner, presentation of all emotional face stimuli was kept brief (100 ms) to ensure that they occurred at specific points in the cardiac cycle. Face stimuli were timed to coincide with the end of cardiac diastole (indexed by the ECG R-wave) and with the end of cardiac systole (approximately at the ECG T-wave), when baroreceptor impulses are processed centrally. Emotion intensity judgments were obtained using a modified forewarned reaction time task (Gray et al., 2012) in which the face cue provided an emotional context for the delayed intensity judgment decision. Each face was kept on the screen for a brief 100 ms period, followed by a 150 ms fixation cross and a "Ready…" preparation signal lasting between 3 and 4 s which was followed by the "GO" command and simultaneous appearance of a visual analog scale (VAS) that subjects used to signal their perceived emotional intensity of the face depicted previously (Fig. 1*C*). The VAS ran from 0 to 50; all values were multiplied by two for display and analysis purposes within the results section. The experiment was separated into two functional runs and each participant had 80 trials (40 fear and 40 neutral faces), half of which were randomized to coincide with systole and the other half diastole.

Anxiety. State anxiety was assessed immediately before the experimental session using the "state" subscale of the Spielberger State-Trait Anxiety Inventory (Spielberger, 1983).

MRI acquisition and preprocessing. Participants underwent structural MRI imaging using a Siemens Avanto 1.5 tesla MRI scanner. Functional echoplanar datasets sensitive to BOLD contrast were acquired with axial slices (anterioposterior phase encode direction) tilted 30 degrees from intercommissural plane to minimize T2* signal dropout from orbitofrontal and anterior temporal regions. Thirty-five 3 mm slices with a 0.75

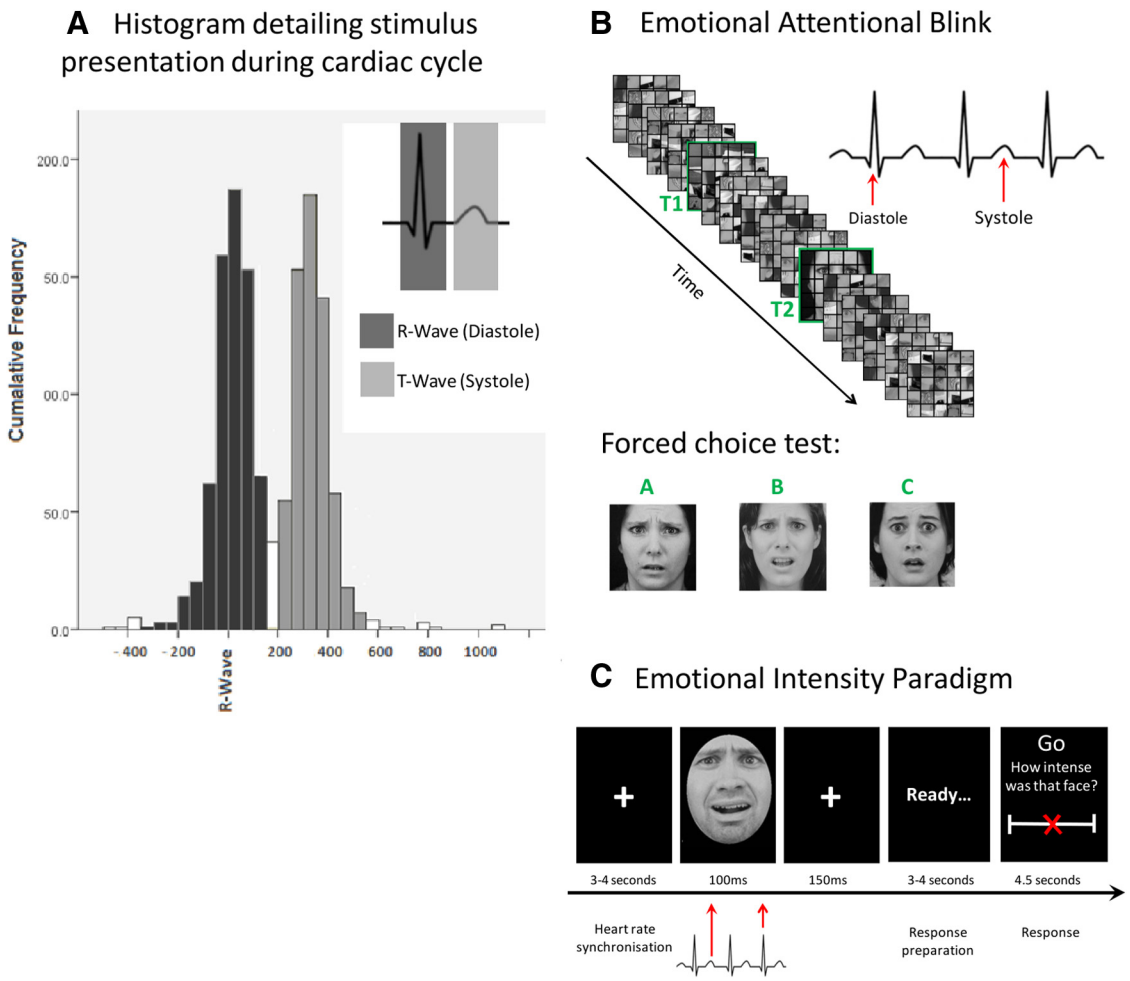

Figure 1. ***A***, Histogram detailing fear and neutral face presentation in relation to cardiac cycle within the MRI scanner. For Experiments 1 and 2, stimulus presentation was time locked to coincide with distinct points of the cardiac cycle. ***B***, For Experiment 1, participants were required to detect two targets (T1 and T2, outlined in green for illustrative purposes in this diagram only) embedded within an RSVP. T2 (face) detection served as the variable of interest, as determined by a subsequent forced-choice recognition test. ***C***, For Experiment 2, face presentation (fear and neutral) were time locked to diastole and systole. Participants made subsequent trial-by-trial emotion intensity judgments using a VAS.

mm interslice gap were acquired, providing full brain coverage with an in-plane resolution of 3 × 3 mm (TE = 42 ms, TR = 2620 ms). Because stimulus presentation was contingent on heart timing, the experiment was variable in duration depending on the individual participant's heart rate. On average, 411 volumes were collected and task duration was 18 min in total, divided into 2 functional runs of ~9 min each (range 8.08–10 min). After acquisition of the functional dataset, full brain T1-weighted structural scans were also acquired from each participant (MPRAGE, 0.9 mm^3 voxels, 192 slices, 1160/4.24 ms TR/TE, 300 ms inversion time, 230 × 230 mm^2 FOV). Images were preprocessed using SPM8 (http://www.fil.ion.ucl.ac.uk/spm/). The initial four functional volumes were discarded to allow for equilibration of net magnetization. Images were then spatially realigned, unwarped, spatially normalized to standard MNI space, and movement regressors were added. Normalized functional scans were smoothed with an 8 mm Gaussian smoothing kernel (Friston et al., 2000).

Data analysis. For Experiment 1, a repeated-measures 2 × 4 ANOVA was conducted to explore the effect of cardiac timing on correct detection of faces during the emotional attentional blink. Heart timing (diastole, systole) × emotion (fear, disgust, neutral, happy) were entered as within-participant variables. The main effect of emotion was broken down using standard *t* tests in accordance with the hypothesis that the detection of emotion items (fear, disgust, and happy) would be enhanced relative to neutral stimuli. The significant cardiac cycle by emotion interaction was explored using *post hoc t* tests corrected for multiple comparisons using the Bonferroni method (*p*-value adjusted based on eight *post hoc* tests). For Experiment 2, we tested for a cardiac induced shift in emotional intensity using a 2 cardiac cycle (diastole, systole) × 2 emotion (neutral, fear) repeated-measures ANOVA on intensity ratings. Standard *t* tests were used to break down significant interactions to pursue our hypothesis of enhanced fear processing at systole.

Functional neuroimaging data were analyzed with the standard hierarchal model approach (Penny and Friston, 2003) and modeled in a stochastic-event-related manner. Individual first-level models were constructed coding for heart timing (diastole, systole), and emotion (fear, neutral). Contrasts were constructed detailing main effects of heart timing (diastole vs systole) and interaction effects (fear diastole − neutral diastole vs fear systole − neutral systole). To correct for multiple comparisons, we conducted 10,000 Monte Carlo simulations using custom software written in MATLAB (Slotnick, 2008). For individual thresholds set at $p < 0.01$, these were corrected for multiple comparisons at the stringent threshold of $p = 0.0001$, limiting analyses to 33 contiguous voxels to avoid type I error rates and to achieve a significance level of $p < 0.05$ (Slotnick and Schacter, 2006; Slotnick, 2010; Thakral, 2011). This correction approximates to a Bonferroni correction. For FWE-corrected ROI analyses, anatomical masks were constructed using the anatomical toolbox in SPM (Tzourio-Mazoyer et al., 2002) for bilateral amygdala, insula, and hippocampus, and a function ROI was constructed for the periaqueductal gray (PAG) using a 7 mm sphere around the coordinates (6, −32, −14; Gray et al., 2012).

Poststimulus time histogram (PSTH) plots were computed with the RFX toolbox implemented in SPM (Gläscher, 2009) using an anatomical ROI of bilateral amygdala to derive peak activity. Stimulus onset was set

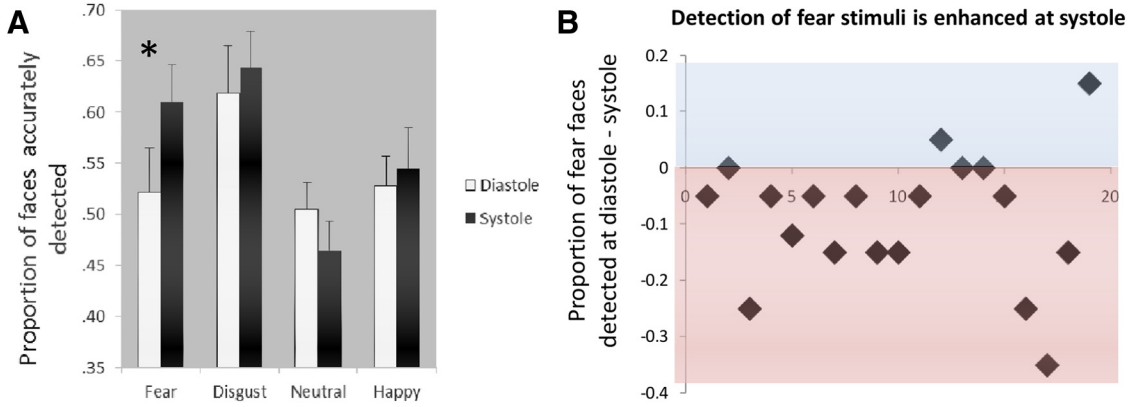

Figure 2. We tested the hypothesis that the cardiac cycle influences the processing of emotional stimuli using an RSVP task to present emotional and neutral stimuli periliminally (i.e., subceiling for detection). We extend the established findings that emotional stimuli are detected (i.e., "break through to awareness") more than neutral stimuli by showing that, for fear faces only, this effect is modulated by the cardiac cycle, with enhanced detection of fear faces observed at systole relative to diastole. All other emotions (happy, neutral, disgust) were not significantly affected by cardiac cycle (***A***). Cardiac modulation of fear detection is documented at the subject level to illustrate individual shifts in fear face detection (each separate subject is represented as a diamond). The *y*-axis represents the percentage of fear faces detected at diastole − systole. The majority of participants were more likely to correctly identify fear faces at systole relative to diastole, as marked by a negative shift (***B***).

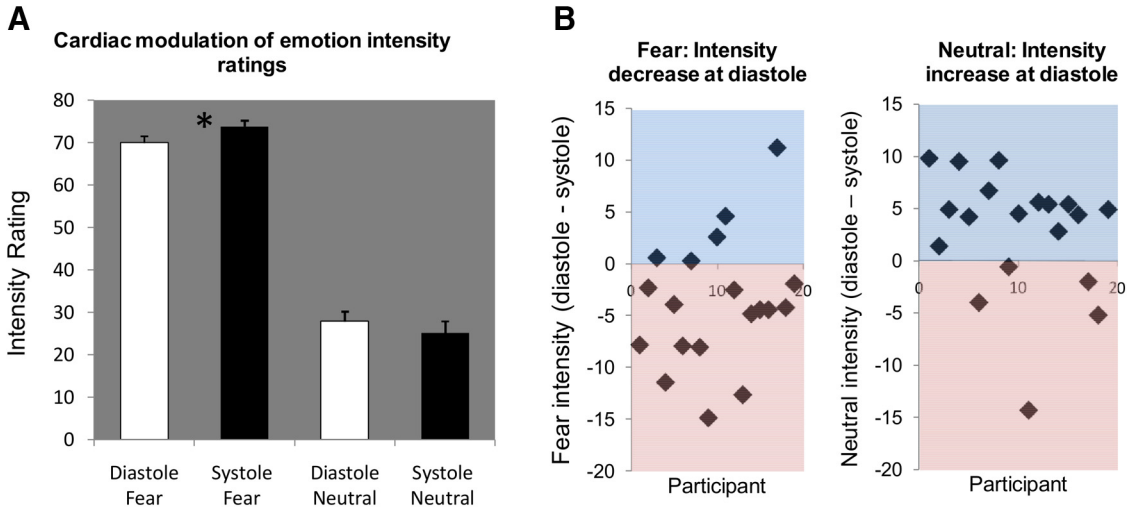

Figure 3. Graph depicting the interaction between cardiac timing and emotion intensity, with an increase in perceived subjective intensity of fear faces at systole and a (nonsignificant) tendency for neutral faces to be perceived as more intense at diastole (***A***). Cardiac modulation of fear intensity documented on the subject level to illustrate individual shifts in perceived fear intensity (each separate subject is represented as a diamond). The *y*-axis represents fear intensity ratings for faces at diastole − systole. The majority of participants were more likely to rate fear faces as more intense if seen at systole relative to diastole, as marked by a negative shift (***B***).

to time 0 and the percent signal change over time was plotted in multiples of TR (2.62 s) separately for fear faces at diastole, neutral faces at diastole, fear faces at systole, and neutral faces at systole.

Results

Experiment 1: behavioral emotional attentional blink (EAB)

A main effect of emotion ($F_{(3,54)} = 8.8$, $p < 0.001$) signaled the emotional blink effect, showing that emotional faces were better identified relative to neutral faces. This effect reached significance for all emotion categories: fear (mean 0.57 ± 0.037) versus neutral faces (mean 0.48 ± .026; $t_{(18)} = 2.6$, $p = 0.019$), disgust (mean 0.63 ± 0.039) versus neutral ($t_{(18)} = 6.0$, $p < 0.001$), and happy (mean 0.53 ± 0.031) versus neutral ($t_{(18)} = 2.1$, $p = 0.046$). There was no overall main effect of cardiac cycle ($F_{(1,18)} = 2.1$, n.s.), indicating that, when collapsed across all emotion categories, items were not better detected at either diastole (mean 0.54 ± 0.03) or systole (mean 0.57 ± 0.031).

We observed a significant cardiac cycle by emotion interaction ($F_{(3,54)} = 3.0$, $p = 0.038$). Therefore, the perception accuracy for fear faces was significantly modulated by cardiac cycle ($t_{(18)} = -3.3$, $p = 0.032$), with a significantly greater detection breakthrough of fear faces occurring at systole (mean 0.61 ± 0.036) relative to diastole (mean 0.52 ± 0.042). No significant detection differences were found between disgust ($t_{(18)} = -0.7$, n.s.; systole mean 0.64 ± 0.036, diastole mean 0.62 ± 0.046), neutral ($t_{(18)} = 1.5$, n.s.; systole mean 0.46 ± 0.029, diastole mean 0.50 ± 0.027), and happy ($t_{(18)} = -0.5$, n.s.; systole mean 0.54 ± 0.039, diastole mean 0.53 ± 0.029) faces as a function of cardiac cycle (Fig. 2).

Perception of fear faces at systole was significantly enhanced relative to neutral faces at both diastole ($t_{(18)} = 3.5$, $p = 0.024$) and systole ($t_{(18)} = 3.4$, $p=0.024$). In contrast, there was no difference in the detection of fear faces at diastole compared with neutral faces either at diastole ($t_{(18)} = 0.2$, n.s.) or systole ($t_{(18)} = 1.0$, n.s.). These findings clarify that the detection advantage normally afforded to fear, relative to neutral, faces was eliminated at diastole.

T1 "breakthrough" (i.e., correct identification of house stimuli) did not differ with our cardiac cycle manipulation. There was

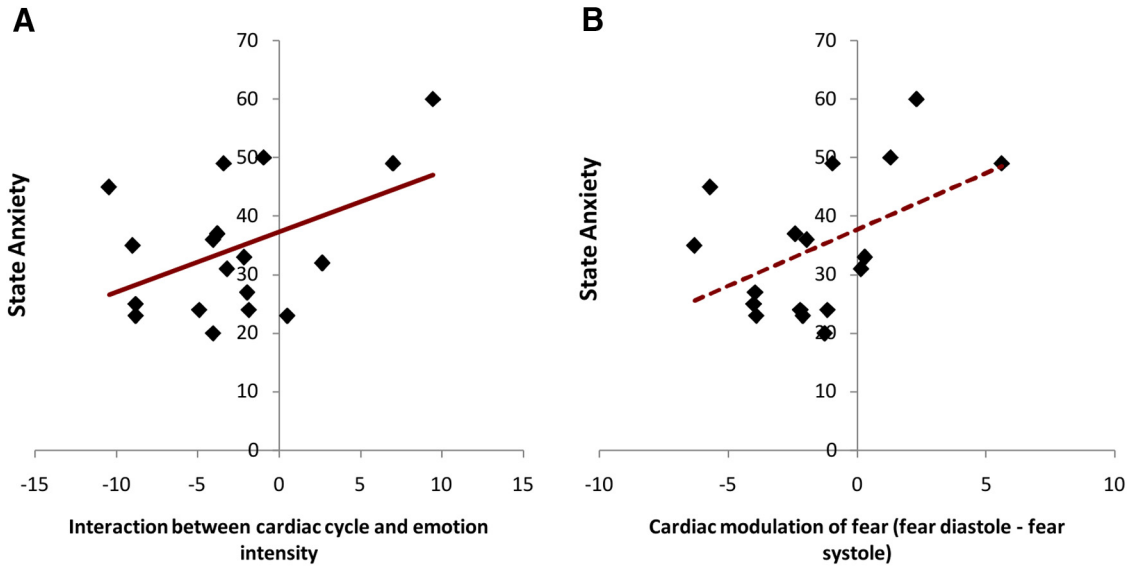

Figure 4. The interaction between cardiac cycle and emotion correlated significantly with state anxiety (***A***). This was largely driven by cardiac modulation of fear (diastole − systole), which displayed a trend relationship with state anxiety (***B***). Therefore, the relative inhibition of threat processing at diastole was aberrant with anxiety, suggesting a potential mechanism contributing to sustained overreactivity to fear signal and threat in anxiety.

no main effect of T1 perception as a function of trials time locked to systole (mean 0.44 ± 0.084) versus diastole (mean 0.44 ± 0.068; $F_{(18)} = 0.3$, $p = 0.619$) and no emotion by cardiac cycle interaction for T1 detection ($F_{(18)} = 0.4$, $p = 0.740$), thus establishing that the effect of the cardiac cycle was specific to T2 fear stimuli.

Experiment 2: cardiac modulation of emotion intensity

When participants viewed supraliminal face stimuli, a main effect of emotion was observed ($F_{(1,18)} = 334.9$, $p < 0.001$), reflecting greater intensity ratings for fear faces relative to neutral faces. There was no overall main effect of cardiac cycle ($F_{(1,18)} = 0.4$, n.s.), signifying that, collapsed across emotion categories, faces presented at diastole were rated equally intense as those on systole. There was, however, a significant cardiac cycle by emotion interaction ($F_{(1,18)} = 8.2$, $p = 0.01$), which reflected the propensity for fear faces to be judged as more intense at systole (mean 73.8 ± 1.42) than at diastole (mean 70.03 ± 1.53; $t_{(18)} = -2.7$, $p = 0.016$). Ratings for neutral faces showed a trend in the opposite direction, where they were more likely to be judged as more intense at diastole (mean 27.93 ± 2.34) relative to systole (mean 25.13 ± 2.82; $t_{(18)} = -2.1$, $p = 0.055$; Fig. 3).

Relationship to anxiety

Individual differences in state anxiety correlated with the magnitude of the behavioral interaction between cardiac cycle and emotion-specific intensity judgments as follows: (fear diastole − neutral diastole) > (fear systole − neutral systole) ($r = 0.5$, $p = 0.041$). This interaction was principally driven by a correlation between the simple effect of cardiac cycle on the perception of fear stimuli (fear at diastole − fear at systole) that was approaching significance ($r = 0.47$, $p = 0.052$). The correlation with neutral stimuli as a function of cardiac timing (neutral at diastole − neutral at systole) was going in the opposite direction, although was nonsignificant ($r = -0.38$, $p = 0.136$). Therefore, background anxiety reduced the attenuation of fear ratings to stimuli presented at diastole (Fig. 4).

Table 1. Main effect of cardiac cycle

Brain area	Side	Coordinates (mm)	Voxels	*t*-score
Diastole > systole				
Parahippocampal gyrus	L	−18, −24, −26	107	5.4
Middle frontal gyrus	L	−24, 14, 46	137	5.3
Anterior insula/Inferior frontal gyrus	L	−34, 20, −6	132	4.7
Middle frontal gyrus	R	50, 8, 40	42	3.6
Middle frontal gyrus	L	−48, 6, 38	54	3.5
Insula	R	34, 12, −14	63	3.4
Angular gyrus	R	58, −48, 34	43	3.4
Parahippocampal gyrus	R	18, −26, −26	34	3.3
Superior frontal gyrus (medial)	R	6, 40, 42	34	3.1
Systole > diastole				
Hippocampal formation	L	−38, −8, −26	124	5.8
Middle insula	L	−34, 4, 2	104	4.9
Inferior occipital gyrus	L	−24, −86, 10	101	4.9
Precentral gyrus	L	−28, −14, 48	97	4.8
Occipital pole	R	32, −90, −20	86	4.3
Precuneus	R	20, −80, 42	82	4.1
Cerebellum	R	22, −64, −38	44	4.0
Angular gyrus	L	−30, −52, 52	50	3.7
Precuneus	L	−20, −92, 28	167	3.6
Cerebellum	R	10, −56, −10	35	3.4

Shown is the brain activation underlying the main effect of cardiac modulation of emotion processing collapsed over specific emotion type.

Neuroimaging findings

Main effect of cardiac cycle

Activity within a set of specific brain regions showed a significant main effect of heart timing during the processing of face stimuli (regardless of emotion; for faces presented at systole > diastole and diastole > systole; Table 1). In particular, subregions of anterior insula (Fig. 5*A*) and prefrontal cortex, medial temporal lobe, and middle frontal gyrus were sensitive to cardiac cycle effects on face processing.

Emotion and cardiac cycle

To investigate how baroreceptor afferent information differentially affected fear processing, we tested for an interaction between cardiac timing and emotion category (for fear systole >

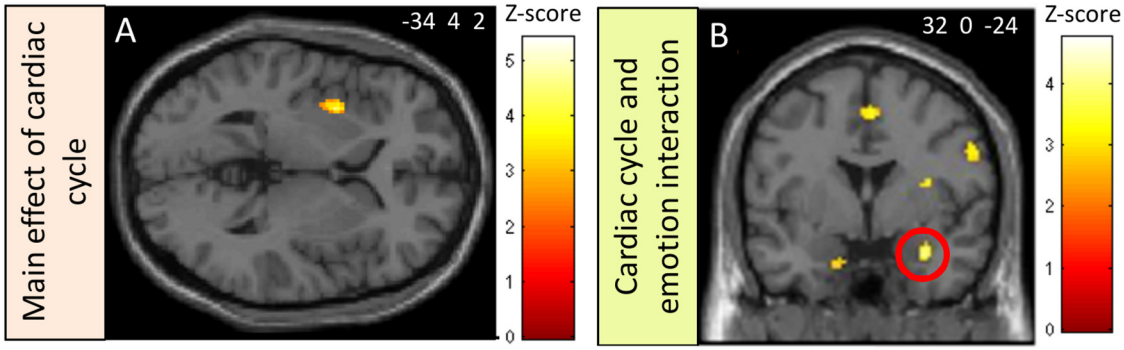

Figure 5. Main effect of cardiac cycle on emotion processing, documenting increased activity in left anterior insula (−34, 4, 2) for faces at systole > diastole (***A***). Brain activity illustrating the interaction of cardiac timing on emotion processing (fear systole > neutral systole vs fear diastole > neutral diastole). Notably, significant activation was observed in bilateral amygdala, with activity in right amygdala meeting FWE correction (circled). See Table 2 for a complete listing of activity during interaction (***B***).

Table 2. Interaction between cardiac cycle and emotion

Brain area	Side	Coordinates (mm)	Voxels	*t*-score
Amygdala	R	32, 0, −24	36	4.3
Cluster incorporating superior temporal gyrus/amygdala	L	−26, 10, −34	156	4.6
Dorsal posterior cingulate cortex	L	−10, −42, 28	123	4.7
Occipital temporal gyrus	R	24, −26, −26	93	4.6
Angular gyrus	L	−34, −54, 40	91	4.4
Supplementary motor area	R	4, −26, 58	66	4.3
Middle cingulate cortex incorporating anterior cingulate	L	−8, −6, 30	36	4.2
Temporal parietal junction	R	40, −46, 20	33	4.2
Precentral gyrus	R	40, −10, 30	42	3.8
Precentral gyrus	R	56, −2, 30	97	3.8
Superior frontal gyrus (medial)	R	12, 28, 48	60	3.8
Anterior insula	R	28, 8, 12	46	3.8
Middle insula	R	32, 0, 14		3.2
Cuneus	L	−4, −78, 20	62	3.7
Superior frontal gyrus (anterior)	L	−14, 62, 28	41	3.6
Temporal pole	R	30, 16, −26	97	3.6
Inferior frontal gyrus pars orbitalis	L	−38, 50, −12	57	3.6
Supplementary motor area	R	2, 0, 52	35	3.4
Middle frontal gyrus (anterior)	L	−40, 52, 18	34	3.4

Shown is the interaction effect of cardiac timing on emotion (fear systole > neutral systole vs fear diastole > neutral diastole).

neutral systole verses fear diastole > neutral diastole; Fig. 5*B*, Table 2). These analyses showed that the response of the amygdala was enhanced to fear stimuli (relative to neutral stimuli) presented at systole compared with diastole. Also consistent with a facilitation of fear processing, insular, extrastriate, motor, and supplementary motor, cingulate and medial temporal lobe cortices also showed corresponding activity changes during this interaction.

A small volume correction in the anatomically defined amygdala ROI revealed that right amgydala activity met this stringent threshold (T = 4.31, 28 voxels, $p = 0.05$ FWE correction). Activity in the left amygdala did not meet reach this criterion (T = 2.94, 3 voxels, n.s.; Fig. 5*B*). We also extracted the mean activation from bilateral anatomical ROIs for offline analyses, which showed that activity within both right ($t_{(18)} = 4.2$, $p = 0.001$) and left ($t_{(18)} = 2.9$, $p = 0.01$) amygdalae manifest the interaction (fear systole > neutral systole vs fear diastole > neutral diastole). The parameter estimates derived from bilateral amygdala demonstrate enhanced activity for the contrast fear systole − fear diastole and hypoactivation for the contrast neutral systole − neutral diastole (Fig. 6*A*). Elevation of the hemodynamic response was observed in bilateral amygdala after fear faces at systole, with attentuation of amygdala activity to fear faces at diastole and neutral faces at systole (illustrated in separate PSTH plots of percentage signal change over time after face presentations; Fig. 6*B*). These observations add to evidence showing the integration of cues concerning environmental threat with information concerning physiological disposition (from cardiac afferent signals) in the human amygdala (Figs. 5*B*, 6*A*,*B*).

A series of additional anatomical small volume corrections were performed in bilateral hippocampus, bilateral insula, and a functional ROI in PAG. None of these ROIs were sensitive to the interaction between cardiac cycle and emotion processing (all FWE $p > 0.2$).

Demographic analyses

When we tested for effects of age and sex on the cardiac modulation of emotion/fear processing, we observed no significant effects of sex on intensity judgments of fear stimuli (i.e., fear systole − fear diastole, for males vs females, $t_{(17)} = 0.4$, $p = 0.69$) or neutral systole − neutral diastole ($t_{(17)} = 0.5$, $p = 0.61$; Experiment 2). Analyses including age as a covariate also did not reveal any additional significant findings. The cardiac modulation of intensity ratings (ratings at diastole − systole) did not correlate with age for fear ($r = -0.3$, $p = 0.289$) or neutral ($r = 0.1$, $p = 0.703$) faces.

Discussion

The neural processing and conscious experience of sensory stimuli are influenced by visceral state. Here, we demonstrate that fear processing is modulated by cardiac timing. Specifically, the processing of fear faces was enhanced at systole and attenuated at diastole. Behaviorally, during an attentional blink task, the detection advantage typically afforded to emotional stimuli was seen for fear faces presented at systole, but was suppressed at diastole. Likewise, intensity ratings of fear faces were significantly greater at systole relative to ratings of fear faces presented at diastole. Using fMRI, we show that activity within regions, notably the amygdala, was sensitive to phase of the cardiac cycle and predicted shifts in emotional judgments timed with natural baroreceptor discharge. Moreover, these effects were weighted by individual differences in the expression of anxiety symptoms. Specifically, the relative inhibition of fear at diastole was perturbed by heightened anxiety, suggesting a potential mechanism through which altered heart–emotion coupling could contribute to sustained threat processing in highly anxious individuals.

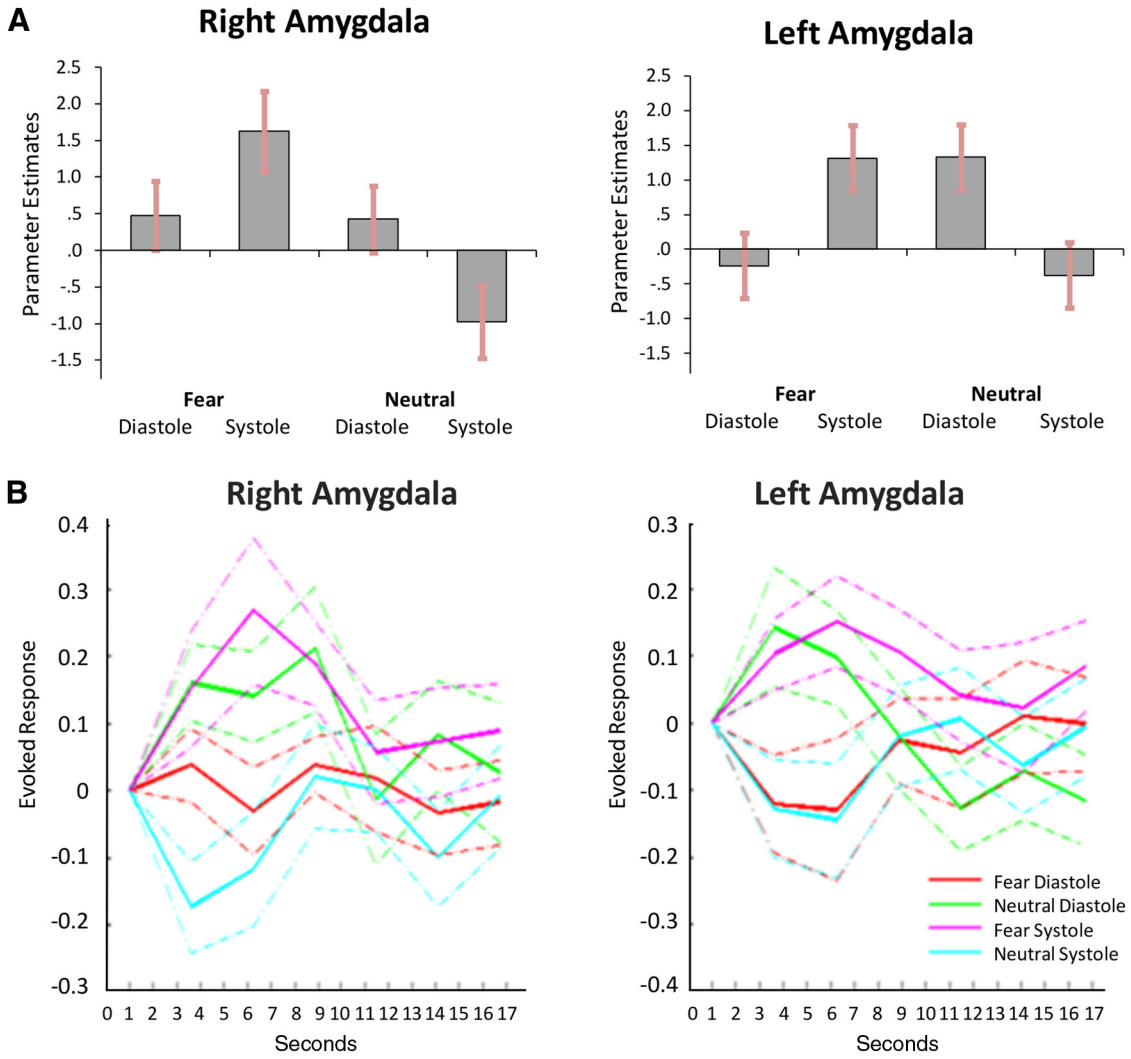

Figure 6. Patterns of bilateral amygdala activity correspond to emotion specific cardiac shifts in intensity, with increases for fear stimuli at systole and increases for neutral faces at diastole. Parameter estimates extracted from peak voxels in right (32, 0, −24) and left (−16, 0, −28) amygdala as defined by the interaction (fear systole > neutral systole vs fear diastole > neutral diastole; ***A***). PSTH plots were computed using an anatomical ROI of bilateral amygdala to derive peak activity. Stimulus onset was set to time 0 and PSC over time was plotted in multiples of TR (2.62 s) separately for fear faces at diastole, neutral faces at diastole, fear faces at systole, and neutral faces at systole (***B***).

These findings provide novel insight into neural mechanisms through which emotion is shaped by bodily state. Importantly, they show a facilitation of fear processing at systole and this observation counters a broad assumption, based on previous studies, that the activation of arterial baroreceptors results in a general inhibition of sensory processing and cortical excitability (Lacey and Lacey, 1970; Gahery and Vigier, 1974; Koriath and Lindholm, 1986). Many of these earlier studies focused on pain processing, noting the attenuation of neurophysiological responses to pain stimuli presented at systole, including dampening of the nociceptive flexion reflex and a reduction in pain evoked potentials. Here, noxious laser stimulation at systole elicits smaller N2-P2 amplitude compared with stimulation at diastole (Edwards et al., 2008), which we interpreted to reflect objective differences in the degree of induced pain. P2 amplitude is also associated with pain anticipation and is larger for cued nociceptive skin stimuli, an effect that is abolished for stimuli presented during baroreceptor activation (Gray et al., 2010).

Our findings therefore refute this notion that there is always an inhibitory effect of systole and baroreceptor afferent firing on the processing of sensory stimuli. We demonstrate that, in the domain of fear, subjective, behavioral, and neural responses are greater at systole and attenuated at diastole. In both of our experiments, there was an effect of enhanced fear processing at systole. Therefore, our behavioral effects are not simply due to an interaction, but have merit in terms of their simple effects, especially with regard to fear. Indeed, our results are consistent with emerging work suggesting exaggerated subjective emotional and neural responses at systole for specific threatening stimuli, illustrated by enhanced amygdala and pontine activation to electric shock at systole (Gray et al., 2009) and augmented ratings of unpleasantness and pain intensity during unpredicted pain stimulation at systole relative to diastole (Martins et al., 2009). We used the attentional blink paradigm as a means of showing cardiac timing (baroreceptor activation) effects on perceptual breakthrough of emotional stimuli. We anticipate that the finding of "systole-enhanced fear perception" generalizes to other masking and attentional tasks sensitive to attentional grab and pop-out effects of emotive stimuli. Nevertheless this prediction needs to be confirmed empirically.

The amygdala is one region involved in translating psychological stress into bodily arousal (Gianaros et al., 2008). Our evi-

dence shows that this relationship is bidirectional. Afferent signals of physiological arousal are represented within the amygdala and integrated with the processing of threat stimuli (Critchley et al., 2002b). Here, we show that this integration is present for viscerosensory signals occurring with each heartbeat to enhance psychological measures of fear intensity. Using the emotional attentional blink paradigm, we also show that detection sensitivity to fear stimuli is modulated as a function of cardiac cycle. This finding informs the interpretation of earlier research also implicating amygdala, which demonstrates that the detection breakthrough of masked stimuli is influenced by emotional state (Anderson and Phelps, 2001) and that the perception of threat relates to the degree of physiological arousal (Lang et al., 2000). Our findings also suggest that cardiac modulation of emotion as mediated through amygdala may display a particular functional specificity to fear stimuli. Breakthrough of emotional stimuli into consciousness within emotional attentional blink tasks is known to be gated by amygdala (Anderson and Phelps, 2001).

Beyond amygdala, our neuroimaging findings provide further insight with respect to the interaction between short-term fluctuations in bodily state and processing of salient emotional stimuli. Regardless of emotional valence (i.e., for both neutral and fear), cardiac timing modulated the pattern of neural responses to face stimuli. Within medial temporal lobe, systole enhanced hippocampal responses and decreased more posterior parahippocampal activity. Systole also enhanced responses within early visual areas and decreased responses within medial prefrontal cortices. Activity within insula was also shifted by the timing of visual stimuli in relation to these phasic internal signals. Speculatively, such effects may subtly alter the degree to which stimuli access conscious awareness. However, within both of our experiments, the behavioral impact emerged only for processing fear relative to neutral faces. This interaction, which clearly involved the amygdala as hypothesized, was also expressed within "viscerosensory" anterior and middle insula, "visual" occipital and temporal areas (implicated in representing salient facial features), and, of particular note, within dorsal posterior cingulate cortex. Arguably, the perceptual interaction with visceral state is tied to "self-representational" default mode processes (this may also account for involvement of regions implicated in somatic self-representation). Whereas amygdala responses tracked cardiac modulation of intensity ratings, activation of other regions in parallel may have "normalized" this activity, particularly pertaining to neutral stimuli, in the production of fear states. This is entirely consistent with a cognitive contextual appraisal of the stimuli that is modulated by physiological signals in a manner that is mediated in part by the amygdala alongside regions such as insula (Critchley et al., 2002b). Cingulate, principally the anterior cingulate cortex, could have served as a punitive source of interoceptive regulation (Medford and Critchley, 2010), along with prefrontal regions involved in emotion regulation, notably superior frontal gyrus (Ochsner et al., 2002).

Delineating the neurocircuitry through which cardiac afferent signaling modulates fear is important for a mechanistic understanding of how physiological arousal interacts with psychological (attentional and emotional) processing. This is particularly relevant to anxiety disorders, which are typically accompanied by enhanced cardiovascular reactivity (Pollatos et al., 2007), increased threat detection (Bradley et al., 1998; Mogg et al., 2004), and hyperactivity of threat-related neurocircuitry such as amygdala (Phan et al., 2006). Indeed, anxiety conditions such as PTSD are characterized by feelings of imminent danger, which prevail even in clear safety contexts (Garfinkel and Liberzon, 2009), contributing to hyperarousal, hypervigilance, and reduced fear inhibition (Jovanovic et al., 2010). Consistent with this, we observed that individual differences in reported anxiety affected the magnitude of the cardiac influence on emotion processing. The shift in fear perception as a function of cardiac cycle was also directly affected by state anxiety, with low anxiety individuals inhibiting fear perception at diastole. This relative inhibition of fear processing at diastole is impaired in individuals with high anxiety, suggesting a potential mechanism that could contribute to sustained fear responding associated with anxiety. This observation links the physiological component of threat processing to the expression of anxiety and, by extension, to the individual's vulnerability to anxiety disorders. Nevertheless, the effects of anxiety on cardiac modulation of emotion, and fear specifically, are at this stage preliminary and require further testing, replication, and extension into clinical populations. Further research is needed to establish whether aberrant interactions among visceral state, brain, and emotion are central to the exaggeration of fear processing in patients with anxiety disorders.

In our experiment, fear was the only emotion for which stimulus detection was reliably affected by cardiac cycle: Fear detection was enhanced at systole, but detection of stimuli conveying disgust and happiness (which can be viewed as valence and intensity controls) were not affected by heart timing. Therefore, the present study demonstrates fear specificity for stimulus detection in relation to the cardiac cycle. Intensity judgment of fear stimuli was also affected by cardiac cycle, but the specificity for this is less clear. In some circumstances, explicit appraisal of disgust faces can be affected by cardiac cycle, but this is not associated with amygdala engagement (Gray et al., 2012). Moreover, our results also point to a less pronounced, opposite effect for neutral stimuli, suggesting that the effect between cardiac cycle and emotion is not a simple monotonic exaggeration of intensity at systole, but rather an interaction with specific emotions. Neutral items tended to be judged as more intense at diastole relative to systole, when amygdala activation was also greater for neutral items at diastole relative to systole. This observation extends previous results reporting changes in intensity and unpleasantness of neutral items across the cardiac cycle (Martins et al., 2009). In anxiety, there is typically an enhanced amygdala response to neutral faces (Somerville et al., 2004). The motivational ambiguity associated with neutral facial expressions can be interpreted as threatening by people with raised negative affectivity, including highly anxious individuals (Gray et al., 2007a). Intact neutral processing is also necessary for the learning of safety signals, which is also impaired in individuals with anxiety (Lohr et al., 2007). Further research is needed to detail how processing of neutral information relates to visceral state, with further implications for understating the mechanisms underlying anxiety.

This is the first work to demonstrate that individual heartbeats improve the perception of fear and intensify the emotional impact of fearful faces, as shown behaviorally and with complementary neuroimaging analyses. This research study was motivated by a desire to understand the contribution of peripheral bodily arousal to emotional experience, particularly fear and anxiety, for which the processing of threat signals has an established relationship to symptom expression. We exploited the phasic nature of cardiac afferent signaling to access the channel of viscerosensory information that encodes the timing and strength of individual heartbeats. Our observations can thus be extrapolated to mecha-

nisms through which general states of cardiovascular arousal (increased heart rate and blood pressure) influence the detection and experience of fear. Research in patients could usefully explore how individual differences in the magnitude of "heart–fear interactions" relate to the clinical expression of anxiety disorders. Ultimately, these findings point to a potential target for novel treatment approaches for the management of anxiety symptoms.

References

Anderson AK, Phelps EA (2001) Lesions of the human amygdala impair enhanced perception of emotionally salient events. Nature 411:305–309. CrossRef Medline

Bechara A, Damasio H, Damasio AR (2000) Emotion, decision making and the orbitofrontal cortex. Cereb Cortex 10:295–307. CrossRef Medline

Bradley BP, Mogg K, Falla SJ, Hamilton LR (1998) Attentional bias for threatening facial expressions in anxiety: manipulation of stimulus duration. Cognition and Emotion 12:737–753. CrossRef

Cahill L, McGaugh JL (1998) Mechanisms of emotional arousal and lasting declarative memory. Trends Neurosci 21:294–299. CrossRef Medline

Critchley HD, Mathias CJ, Dolan RJ (2002a) Fear conditioning in humans: the influence of awareness and autonomic arousal on functional neuroanatomy. Neuron 33:653–663. CrossRef Medline

Critchley HD, Melmed RN, Featherstone E, Mathias CJ, Dolan RJ (2002b) Volitional control of autonomic arousal: a functional magnetic resonance study. Neuroimage 16:909–919. CrossRef Medline

De Martino B, Kalisch R, Rees G, Dolan RJ (2009) Enhanced processing of threat stimuli under limited attentional resources. Cereb Cortex 19:127–133. CrossRef Medline

Domschke K, Stevens S, Pfleiderer B, Gerlach AL (2010) Interoceptive sensitivity in anxiety and anxiety disorders: an overview and integration of neurobiological findings. Clin Psychol Rev 30:1–11. CrossRef Medline

Edwards L, McIntyre D, Carroll D, Ring C, Martin U (2002) The human nociceptive flexion reflex threshold is higher during systole than diastole. Psychophysiology 39:678–681. CrossRef Medline

Edwards L, Ring C, McIntyre D, Carroll D, Martin U (2007) Psychomotor speed in hypertension: effects of reaction time components, stimulus modality, and phase of the cardiac cycle. Psychophysiology 44:459–468. CrossRef Medline

Edwards L, Inui K, Ring C, Wang X, Kakigi R (2008) Pain-related evoked potentials are modulated across the cardiac cycle. Pain 137:488–494. CrossRef Medline

Edwards L, Ring C, McIntyre D, Winer JB, Martin U (2009) Sensory detection thresholds are modulated across the cardiac cycle: evidence that cutaneous sensibility is greatest for systolic stimulation. Psychophysiology 46:252–256. CrossRef Medline

Ekman P, Friesen WV (1974) Detecting deception from body or face. Journal of Personality and Social Psychology 29:288–298. CrossRef

Fredrikson M, Furmark T, Olsson MT, Fischer H, Andersson J, Långström B (1998) Functional neuroanatomical correlates of electrodermal activity: a positron emission tomographic study. Psychophysiology 35:179–185. CrossRef Medline

Friston KJ, Josephs O, Zarahn E, Holmes AP, Rouquette S, Poline J (2000) To smooth or not to smooth? Bias and efficiency in fMRI time-series analysis. Neuroimage 12:196–208. CrossRef Medline

Gahery Y, Vigier D (1974) Inhibitory effects in the cuneate nucleus produced by vago-aortic afferent fibers. Brain Res 75:241–259. CrossRef Medline

Garfinkel SN, Liberzon I (2009) Neurobiology of PTSD: a review of neuroimaging finding. Psychiatric Annals 39:370–381. CrossRef

Garfinkel SN, Barrett AB, Minati L, Dolan RJ, Seth AK, Critchley HD (2013) What the heart forgets: Cardiac timing influences memory for words and is modulated by metacognition and interoceptive sensitivity. Psychophysiology 50:505–512. CrossRef Medline

Gianaros PJ, Sheu LK, Matthews KA, Jennings JR, Manuck SB, Hariri AR (2008) Individual differences in stressor-evoked blood pressure reactivity vary with activation, volume, and functional connectivity of the amygdala. J Neurosci 28:990–999. CrossRef Medline

Gläscher J (2009) Visualization of group inference data in functional neuroimaging. Neuroinformatics 7:73–82. CrossRef Medline

Gray MA, Harrison NA, Wiens S, Critchley HD (2007a) Modulation of emotional appraisal by false physiological feedback during fMRI. PLoS One 2:e546. CrossRef Medline

Gray MA, Taggart P, Sutton PM, Groves D, Holdright DR, Bradbury D, Brull D, Critchley HD (2007b) A cortical potential reflecting cardiac function. Proc Natl Acad Sci U S A 104:6818–6823. CrossRef Medline

Gray MA, Rylander K, Harrison NA, Wallin BG, Critchley HD (2009) Following one's heart: cardiac rhythms gate central initiation of sympathetic reflexes. J Neurosci 29:1817–1825. CrossRef Medline

Gray MA, Minati L, Paoletti G, Critchley HD (2010) Baroreceptor activation attenuates attentional effects on pain-evoked potentials. Pain 151:853–861. CrossRef Medline

Gray MA, Beacher FD, Minati L, Nagai Y, Kemp AH, Harrison NA, Critchley HD (2012) Emotional appraisal is influenced by cardiac afferent information. Emotion 12:180–191. CrossRef Medline

James W (1890/1950) The principles of psychology. New York: Dover Publications.

Jovanovic T, Norrholm SD, Blanding NQ, Davis M, Duncan E, Bradley B, Ressler KJ (2010) Impaired fear inhibition is a biomarker of Ptsd but not depression. Depress Anxiety 27:244–251. CrossRef Medline

Koriath JJ, Lindholm E (1986) Cardiac-related cortical inhibition during a fixed foreperiod reaction time task. Int J Psychophysiol 4:183–195. CrossRef Medline

Lacey I, Lacey BC (1970) Some autonomic-central nervous system interrelationships. In: Physiological correlates of emotion (Black P, ed), pp 205–222. New York: Academic.

Lang PJ, Davis M, Ohman A (2000) Fear and anxiety: animal models and human cognitive psychophysiology. J Affect Disorders 61:137–159. CrossRef Medline

Lange C, ed (1885) The emotions. Baltimore: Williams and Wilkins.

LeDoux JE (2000) Emotion circuits in the brain. Annu Rev Neurosci 23:155–184. CrossRef Medline

Lohr JM, Olatunji BO, Sawchuk CN (2007) A functional analysis of danger and safety signals in anxiety disorders. Clin Psychol Rev 27:114–126. CrossRef Medline

Lundqvist D, Flykt A, Öhman A (1998) The Karolinska directed emotional faces–KDEF, CD ROM from Department of Clinical Neuroscience, Psychology section: Karolinska Institutet, ISBN 91-630-7164-9.

Martins AQ, Ring C, McIntyre D, Edwards L, Martin U (2009) Effects of unpredictable stimulation on pain and nociception across the cardiac cycle. Pain 147:84–90. CrossRef Medline

Medford N, Critchley HD (2010) Conjoint activity of anterior insular and anterior cingulate cortex: awareness and response. Brain Struct Funct 214:535–549. CrossRef Medline

Metzger LJ, Orr SP, Berry NJ, Ahern CE, Lasko NB, Pitman RK (1999) Physiologic reactivity to startling tones in women with posttraumatic stress disorder. J Abnorm Psychol 108:347–352. CrossRef Medline

Mogg K, Philippot P, Bradley BP (2004) Selective attention to angry faces in clinical social phobia. J Abnorm Psychol 113:160–165. CrossRef Medline

Ochsner KN, Bunge SA, Gross JJ, Gabrieli JD (2002) Rethinking feelings: An fMRI study of the cognitive regulation of emotion. J Cogn Neurosci 14:1215–1229. CrossRef Medline

Penny W, Friston K (2003) Mixtures of general linear models for functional neuroimaging. IEEE Trans Med Imaging 22:504–514. CrossRef Medline

Phan KL, Fitzgerald DA, Nathan PJ, Tancer ME (2006) Association between amygdala hyperactivity to harsh faces and severity of social anxiety in generalized social phobia. Biol Psychiat 59:424–429. CrossRef Medline

Pollatos O, Herbert BM, Kaufmann C, Auer DP, Schandry R (2007) Interoceptive awareness, anxiety and cardiovascular reactivity to isometric exercise. International Journal of Psychophysiology 65:167–173. CrossRef Medline

Schachter S, Singer JE (1962) Cognitive, social, and physiological determinants of emotional state. Psychol Rev 69:379–399. CrossRef Medline

Seth AK (2013) Interoceptive inference, emotion, and the embodied self. Trends Cogn Sci 17:565–573. CrossRef Medline

Slotnick SD (2008) https://www2.bc.edu/~slotnics/scripts.htm.

Slotnick SD (2010) Synchronous retinotopic frontal-temporal activity during long-term memory for spatial location. Brain Res 1330:89–100. CrossRef Medline

Slotnick SD, Schacter DL (2006) The nature of memory related activity in early visual areas. Neuropsychologia 44:2874–2886. CrossRef Medline

Somerville LH, Kim H, Johnstone T, Alexander AL, Whalen PJ (2004) Human amygdala responses during presentation of happy and neutral faces: correlations with state anxiety. Biol Psychiat 55:897–903. CrossRef Medline

Spielberger C (1983) Manual for the State-Trait Anxiety Inventory, revised edition. Palo Alto, CA: Consulting Psychologists.

Strack F, Martin LL, Stepper S (1988) Inhibiting and facilitating conditions of the human smile: a nonobtrusive test of the facial feedback hypothesis. J Pers Soc Psychol 54:768–777. CrossRef Medline

Thakral PP (2011) The neural substrates associated with inattentional blindness. Conscious Cogn 20:1768–1775. CrossRef Medline

Tsunoda T, Yoshino A, Furusawa T, Miyazaki M, Takahashi Y, Nomura S (2008) Social anxiety predicts unconsciously provoked emotional responses to facial expression. Physiol Behav 93:172–176. CrossRef Medline

Tzourio-Mazoyer N, Landeau B, Papathanassiou D, Crivello F, Etard O, Delcroix N, Mazoyer B, Joliot M (2002) Automated anatomical labeling of activations in SPM using a macroscopic anatomical parcellation of the MNI MRI single-subject brain. Neuroimage 15:273–289. CrossRef Medline

Zhang ZH, Dougherty PM, Oppenheimer SM (1998) Characterization of baroreceptor-related neurons in the monkey insular cortex. Brain Res 796:303–306. CrossRef Medline